

Effect of Variable Frequency Drive and Pipe Materials on Guava Juice Flow

Shereen S Shalaby^{1*}, Mubarak M Mustafa¹, Yehia A Heikal², Mahmoud Z El Attar¹

1- Agricultural Engineering Dept, Fac of Agric, Ain Shams Univ, P.O. Box 68, Hadayek Shoubra 11241, Cairo, Egypt

2- Food Sciences and Technology Dept, Fac of Agric, Ain Shams Univ, P.O. Box 68, Hadayek Shoubra 11241, Cairo, Egypt

*Corresponding author: shereen_shalaby@agr.asu.edu.eg

<https://doi.org/10.21608/AJS.2022.115676.1453>

Received 10 January 2022; Accepted 28 March 2022

Keywords:

Pressure drop,
Pipe flow,
Variable frequency drive,
Reynolds number,
Rheological properties,
Guava juice

Abstract: In this study, a designed variable frequency drive (VFD) was used to control a single-phase induction motor's speed to pump guava juice at two solid concentrations (9°Bx and 11°Bx). Next, the pressure drop was measured in stainless-steel pipes of three diameters. The pressure drop percentage difference before and after using the VFD at varied flow rates with 10 repetitions at 5-minute intervals was evaluated. The pressure drop reduction range was 19.7%–30.8% and 19.2%–32.4% for the 9% and 11% solid concentrations respectively after using the VFD, which resulted in an average of 25.73% reductions in pressure drop and the pump's total head and driving power. The rheological properties of guava juice were investigated at various temperatures (5, 15, 25, 35, 55 and 75°C). From the results, all materials exhibited non-Newtonian pseudoplastic behavior at all temperatures and concentrations, and correlated well with the power law model, with flow behavior index (n) values less than unity for the 9% and 11% solid concentrations. The findings offer helpful information for predicting how heat variations during processing influence the behavior of guava juice concentrates.

1 Introduction

Estimating pressure drop is critical for evaluating hydraulic requirements in pipe flow, sizing transportation pumps properly, and selecting fittings and tube bending in food processing plants and other areas to reduce operational costs. The friction factor determines the pressure loss in pipes with completely formed regions (Sorgun and Ulker 2020).

For laminar flow, friction factor correlations can be obtained experimentally using a tube's pressure drop over a certain distance or through

the recorded radial velocity profile. Taler (2016) showed that the flow behavior index and Reynolds number significantly affect friction factor predictions.

Centrifugal pumps are used in several fields that require non-Newtonian fluids, such as the food processing and pharmaceutical industries. The shear rate, pressure, and temperature of a non-Newtonian fluid determine its viscosity, which is several orders of magnitude higher than that of water. When the viscosity of a fluid is high, the pump performance is poor compared with water. Moreover, non-Newtonian fluid pumping and mixing require a thorough examination of the fluid dynamic processes occurring

within the used machines. To establish the benefits of centrifugal pump applications, a specialized design approach should consider these consequences (Aldi et al 2017).

A variable frequency drive (VFD) is an adjustable speed drive that modifies an alternating current motor's speed and torque by modifying the motor's input frequency and voltage (Garud et al 2016).

The use of a VFD allows a pump to begin gently. When a VFD is used, the pump motor's energy usage reduces, making it more effective. Particularly, using a VFD decreases switching losses and boosts operating speed, thereby making motor performance very dependable (Prajapati et al 2019).

Losses in a valve-controlled system occur within the valve, and extra piping must bring the valve to any location it is adjusted. With the VFD, no valve losses occur. With no pipe bends needed for a valve, pipe losses are reduced. By eliminating pipe and valve losses, a smaller pump will typically be used. Users can achieve comparable results in flow rates and pressure with a lower power pump (Tahara 2016).

Losses in non-Newtonian fluids have been frequently studied using new definitions of the friction factor or Reynolds number (Johnson et al 2018). The generalized Reynolds number has been applied to the power law, Bingham plastic, and Herschel Bulkley fluids. Csizmadia and Till (2018) proved that among the various available definitions, the generalized Reynolds number (Re_{gen}) correctly arranges the friction factor values.

Abdullah et al 2018 Conducted a flow test using a rheometer to elucidate the flow behavior of pink-fleshed guava, pink-fleshed pomelo, and soursop juice concentrates. To estimate rheological behavior from various temperatures and concentrations, the power law model was used, and a curve was generated by the shear rate–temperature concentration overlap technique. The final equations showed a shear-thinning behavior of pink-fleshed guava, pink-fleshed pomelo, and soursop with flow behavior indices of 0.2217, 0.7507, and 0.6347, respectively.

In this study, we evaluated pressure drop, considering the pipe material and pump velocity, and investigated the influence of temperature on the rheological characteristics of guava juice.

2 Materials and Methods

2.1 Guava juice processing

Ripe guava fruits (*Psidium guajava* L.) were obtained from Cairo Governorate, Egypt, in the 2020-2021 season. The fruits were washed with water and sliced into small pieces. Next, we used a blender to extract the juice directly to remove stone cells, avoid coarse pulp particles, and only have small particles of colloidal consistency. Then, the juice was filtered through a stainless-steel strainer with a mesh value of 24 (1.06 mm diameter) to obtain the juice with a 1 mm average particle size. A rotary evaporator was used to concentrate the juice. Water was added to the samples to produce juices with 9° Bx and 11° Bx. Then, the juices' pH was measured using a calibrated digital pH meter at room temperature; the pH increased to 3.7 after adding 0.14 and 0.15 w/v % of citric acid to the two concentrates. The extracted juices were stored at 4°C until used (Zainal et al 2000).

2.2 Chemical and physical properties

The chemical and physical properties of the juice samples were analyzed using standard methods for soluble solids and acidity, according to (A.O.A.C. 2005).

The total acidity was determined in the juice samples as (%), and the total soluble solid content was determined using a universal laboratory refractometer (Atago No1, 0-32 Brix, Tokyo Japan) at room temperature.

2.3 Density

A specific gravity bottle was used to determine density, according to Earle (1985).

Density = specific gravity of juice × water density at an exact temperature;

The specific gravity of juice = weight of juice ÷ weight of the same volume of water at an exact temperature.

2.4 Rheological measurements

Rheological experiments were conducted at the Rheology Laboratory of the Food Technology Research Institute, ARC, Giza, Egypt (30°01'26.9"N 31°12'29.7"E). The rheological characteristics of the juice samples at various solid concentrations (9°Bx and 11°Bx) were measured at different temperatures (5°C, 15°C, 25°C, 35°C, 55°C, and 75°C) and shear rates (13.2–132). The equipment used was Brookfield AMETEK (Type DVN ext.) (Fig 1). The samples were placed in a small adaptor, and the temperature

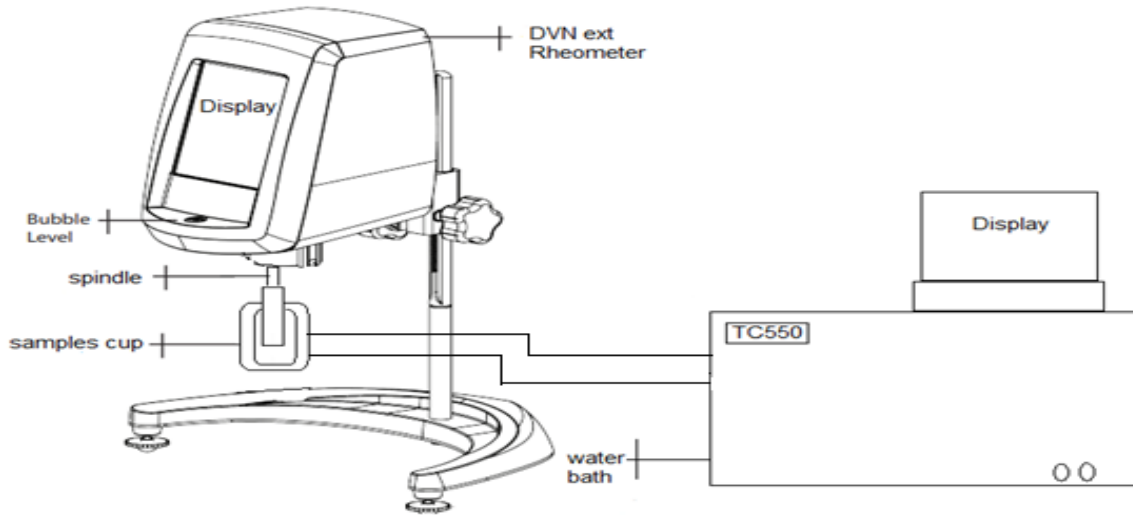


Fig 1. Diagram of the Brookfield Engineering laboratories' DVN rheometer

was maintained using a circulating water bath. For measurements, the SC4-18 spindle was selected, and the rheological parameters were collected directly from the rheometer's software. Then, the stress-strain rate curves were drawn, and the correlation coefficient (R^2) for the rheological model was obtained from the curves.

2.4.1 Power law relations

The power law model, Eq. (1), is used extensively as the empirical model for non-Newtonian fluids in engineering applications; it indicates the flow characteristics of fluids. It matches the testing results for guava, soursop, and pomelo juice concentrates (Quek et al 2013, Abdullah et al 2018).

$$\tau = k \gamma^n, \quad (1)$$

where τ is the shear stress (Pa),

k is the consistency coefficient (pa. s^n),

γ is the shear rate (s^{-1}),

and n is the behavior index.

2.5 Pressure loss measurements in pipe flow

The pressure drop was measured in acrylic and stainless-steel pipes using the apparatus shown in Fig (2). The experimental setup includes a 15-l plastic tank, a water outlet drain at the bottom, and circular tubes (acrylic and stainless-steel) with three nominal sizes (12, 20, and 25 mm). A

centrifugal pump with a power supply (220 V, 50 Hz, 2850 RPM, 0.3HP, flow rate of 20 L/min) was used. Pressure taps (piezometric ring) were installed in the tube test section. A liquid head manometer measured the pressure drop in the straight pipe section of 1.2 m for the acrylic and stainless-steel pipes at flow rates of 3, 4.5, 6, 9, and 10.8 L/m, with 10 repetitions at 5-minute intervals. The flow rate was calculated by weighing the juice samples obtained at predetermined intervals using a stopwatch (0.01 s accuracy). The flow rate was regulated using two methods, as follows:

- a- A throttling ball valve is placed at the pump outlet to obtain the required flow rate under the full operation of the pump motor.
- b- AVFD is attached to the motor to reduce the rotational speed of the driving axes, the impeller rotational speed, and the flow rate of the fluid without implementing a flow regulation valve.

2.6 Friction factors assessment

Equation (2) defines the Fanning friction factor f_{exp} of a viscous fluid flowing in a pipe with a circular cross-section for pressure loss (Sahin and Sumnu 2006)

$$f_{exp} = 2 \Delta P D / \rho \bar{V}^2 L, \quad (2)$$

where ρ is the fluid density ($kg.m^{-3}$),

\bar{V} is the average flow velocity ($m.s^{-1}$),

D is the tube diameter (m),

and Δp is the pressure drop (Pa).

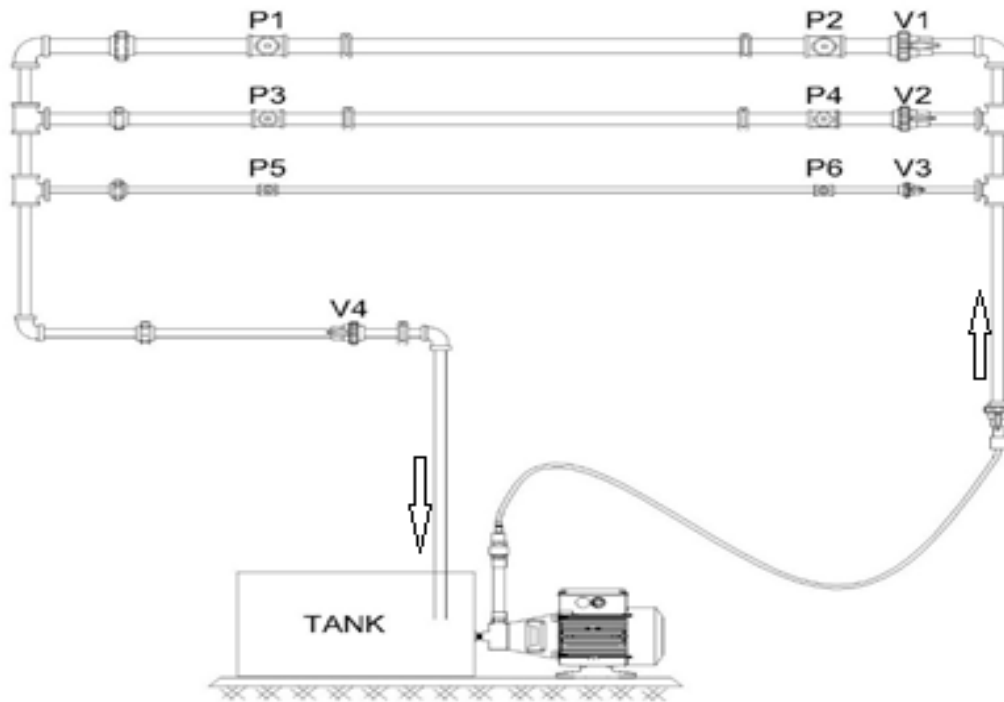


Fig 2. A diagram of the experimental setup, (V: valves, P: piezometric ring. V1, V2, V3, and V4 are, respectively, valves for closing or opening flow through the P1, P2, P3, and P4 test pipes, which are piezometric rings with level-indicating host tubes)

A comparable version of the Hagen–Poiseuille equation for laminar pipe flow of power-law fluids is used to obtain the theoretical friction factor, as applied by (Darby 2001):

$$f_{theo} = 64/R_e, \quad (3)$$

where f_{theo} is the theoretically calculated friction factor, and R_e is the Reynolds number.

The generalized Reynolds number defined by Metzner and Reed (1955) for the power law model for circular pipes can solve the mathematical equation analytically.

$$Re_{mr} = [\rho \bar{V}^{2-n} D^n / 8^{n-1} K] [4n/1 + 3n]^n, \quad (4)$$

where K is the consistency coefficient (Pa. s^n), n is the flow behavior index,

ρ is the fluid density (kg. m^{-3}),

\bar{V} is the average flow velocity (m. s^{-1}),

and D is the tube diameter, (m)

2.7 VFD

In **Fig (3)**, a designed VFD was used to adjust the speed of a single-phase induction motor to

manage the rotational speed of the centrifugal pump [**Fig (3.1)**]. **Table 1** shows the VFD’s specifications. This VFD changed the rotational speed of the motor to the same flow rates of 3, 4.5, 6, 9, and 10.8 L/m by changing the frequency to 11.8, 23.2, 36.4, 43.7, and 50 Hz, respectively. The pressure loss was first measured in three diameters of the stainless-steel pipes using a throttling valve and then compared with the pressure loss when using the VFD for the same pipes.

2.8 Statistical analysis

All statistical data analyses were conducted using SAS software, and an analysis of variance was conducted. The LSD, LSR, and HSD T-tests were used to determine whether there were significant differences between the means ($p \leq 0.05$).

3 Results and Discussion

3.1 Guava juice chemical and physical properties

Table 2 shows the total soluble content and total acidity of the guava juice samples. The total acidity expressed values after adjusting the juice’s pH values in the experiments to 3.7. All values of the tested parameters (viscosity and pressure drop) increased as the total solid content of juice increased.

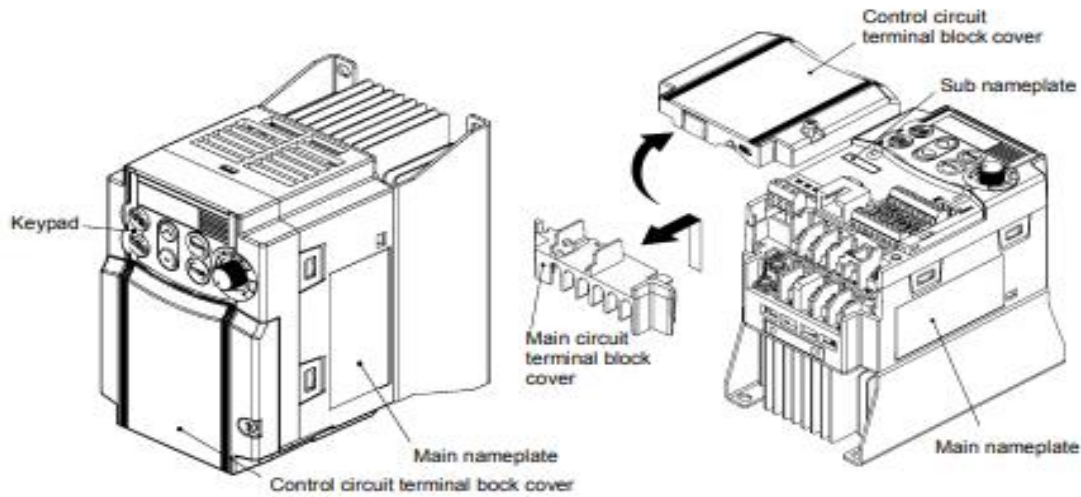


Fig 3. Block illustration of VFD (FVRO-4E11S-7EN model, Fuji Electric co., Ltd)

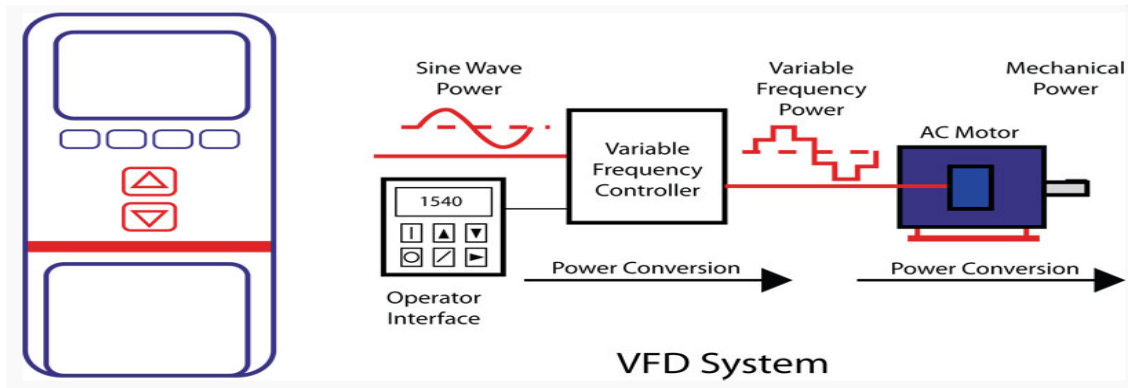


Fig 3.1 Diagram of VFD system (Gopalkrishna et al 2018)

Table 1. Specifications of the variable frequency drive (VFD)

Type	FVR 0.4 E11S-7 EN FVR: Product name 0.4 :Nominal applicable motor capacity: 0.4 kw E11S: Series name 7: Power voltage system: 7: Single-Phase 4: Three-Phase EN: Version
Source	1Phase: 200 – 240 V, 50/60 Hz, 6.4 A
Output	3Phase: 0.4 kw, 200 – 230V, 0.2 – 400Hz, 3A
Serial. No	010113R0001

Table 2. Chemical and physical characteristics and density of guava juice samples

Parameter	Concentrations of guava juice	
	9°	11°
TSS (°Bx)	9°	11°
Total acidity %	3.64	3.7
density (kg.m ⁻³)	980	1050

3.2 Rheograms

Rheograms representing the flow curves of guava juice (9° Bx and 11° Bx) were measured at different temperatures. The results indicate that all samples exhibited non-Newtonian pseudoplastic behavior for all concentrations and temperatures. Shear stress was obtained as a nonlinear function of the shear rate. The shear stress increased with the shear rate at all temper-

atures and concentrations. The observed stress-strain rate data were well-correlated with the pseudoplastic type [Eq. (1)]. The correlation coefficient (R^2) ranged between 0.9845 and 0.9998. **Table 3** shows the flow behavior indicator (n) and consistency coefficient (K) determined from the graphs of the shear stress and shear rate for the two concentrations. In all cases, the juice showed pseudoplastic behavior because the flow index (n) was less than unity.

3.2.1 Influence of temperature on the apparent viscosity of guava juice

In **Table 3**, the consistency coefficient (K) values of the juice decreased as the temperature increased, whereas the flow behavior index (n values) increased with temperature for both tested concentrations (9° Bx and 11° Bx). However, increasing the concentration from 9° Bx to 11° Bx in K values and reduced n values by more than two folds. For a better comparison of rheological data, a single value for the apparent viscosity was calculated at a selected shear rate of 80 s^{-1} , according to Eq. (5) reported by Sugai (2002). **Table 3** shows the corresponding values, which are also illustrated in **Fig (7)**. The μ_a values followed the same trend as the K values.

$$\mu_a = k \gamma^{n-1}, \quad (5)$$

Where μ_a is the apparent viscosity (Pa.s),

γ is the shear rate (s^{-1}),

and k is the consistency coefficient ($\text{pa} \cdot \text{s}^n$)

3.3 Variation in pressure drop across acrylic and stainless-steel pipes using a throttling valve

Figs 8 and 9 show the relationship between the pressure drop and flow rate of the juice based on data obtained from pressure taps across three diameters (25, 20, and 12 mm) for acrylic and stainless-steel pipes at different flow rates (3, 4.5, 6, 9 and 10.8 L/m). As shown in the graphs, as the pipe diameter increased, the pressure drop decreased. The figures indicate that the pressure drop in acrylic pipes was lower than that in stainless-steel pipes, with average differences ranging from 30.9 % to 38.1%. This could be due to the roughness of the pipe walls of small-diameter pipes, which has a significant impact on the pressure loss of the fluid passing through them (Yuan et al 2016).

3.3.1 Effect of using VFD on pressure drop

Figs 10 and 11 illustrate the effect of using VFD on pressure drop. **Table 4** summarizes the percentage difference in pressure drop before and after using VFD with stainless-steel pipes at each flow rate. The results revealed that using VFD in the hydraulic system reduces the pressure drop (head) and pumping power by 19.2% – 32.4% for the juice samples according to the applied flow rate and pipe diameter. These results agree with those reported by Neuberger and Weston (2012) and Tamminen et al (2014). According to the efficiency charts and affinity equations of centrifugal pumps, a throttling valve will reduce the flow rate, but the centrifugal pump itself operates at full power demand. Using VFD will adapt the rotational speed to the required flow rate by lowering the rotational speed (N). Because the energy savings are proportional to the cube of the speed, under these circumstances, the energy savings from installing a VFD will be considerable.

3.4 Reynolds number influence on fanning friction factor

Using the flow parameters and viscosity of the juice and the tube system's diameter, the Reynolds numbers of the different experiments were calculated according to Eq. (5). The friction factors values (f) were calculated according to Eq. (3), which are listed in **Table 5**. **Figs 12 and 13** show the relationship between the applied Reynolds number and the obtained friction factors for guava juice. The figures show that for small Reynolds numbers, the stronger the shear-thinning effects are, the higher the f_{exp} values are, whereas the converse is true for high Reynolds numbers. In **Table 5**, the Reynolds number of the juice samples ranged between 33.6 and 4,429 according to the applied flow rate, pipe diameter, and concentration. Even at high flow rates (9 and 10.8 L/m), the data show that the flow is in the laminar/transition region. Additionally, there was no significant difference between the experimental friction factor values of acrylic and stainless-steel pipes. However, the 9° Bx and 11° Bx juice sample's friction differed significantly, indicating the significant effect of concentration on transport pumps' friction losses and power sizing. The obtained results agree with those for soursop, pineapple, and sugarcane juices reported by Gratao et al (2007), Cabral et al (2010), and Astolfi-Filho et al (2011), respectively.

Table 3. Values of consistency coefficient (*K*) and flow behavior index (*n*) of guava juice at different temperatures

Temp. (°C)	Concentration					
	9°Bx			11°Bx		
	<i>K</i>	<i>n</i>	$\mu_a \alpha \tau \gamma = 80 \text{ s}^{-1}$	<i>K</i>	<i>v</i>	$\mu_a \alpha \tau \gamma = 80 \text{ s}^{-1}$
5	0.185	0.610	0.0335	0.718	0.483	0.0745
15	0.101	0.677	0.0245	0.311	0.515	0.0490
25	0.057	0.730	0.0175	0.305	0.548	0.0421
35	0.038	0.733	0.0118	0.276	0.556	0.0394
55	0.028	0.767	0.0100	0.251	0.571	0.0383
75	0.016	0.779	0.0061	0.212	0.584	0.0342

Table 4. The percentage difference in pressure drops (*K* pa) of guava juice (9 °Bx and 11°Bx) before and after using the VFD with stainless-steel pipes

Flow rate (L/m)	Diameter (mm)	9°Bx			11°Bx		
		Pressure drop value with VFD	Pressure drop value without VFD	Pressure drop reduction	Pressure drop value with VFD	Pressure drop value without VFD	Pressure drop reduction
3	25	1.7987	2.5957	30.7%	1.9262	2.6987	28.6%
	20	2.2909	2.9226	21.6 %	2.5957	3.7044	29.9%
	12	2.7453	3.6244	24.3%	3.1932	4.7231	32.4%
4.5	25	2.1299	3.0764	30.8%	2.2970	3.1385	26.8%
	20	2.8495	3.5474	19.7%	3.0902	4.1983	26.4%
	12	3.1903	4.2781	25.4%	3.91419	5.2479	25.4%
6	25	2.4803	3.5090	29.3%	2.9356	3.8073	22.9%
	20	3.2565	4.0858	20.3%	3.8421	4.7539	19.2%
	12	3.6825	4.9415	25.5%	4.5219	6.0094	24.8%
9	25	3.1726	4.4608	28.9%	3.6052	5.0524	28.6%
	20	4.0378	5.2876	23.6%	4.5322	6.0711	25.3%
	12	4.2979	5.9702	28%	5.3357	7.203	25.9%
10.8	25	3.7494	4.9992	25%	4.2438	5.7521	26.2%
	20	4.6723	6.0567	22.9%	5.2533	6.91488	24%
	12	4.9227	6.7873	27.5%	6.3863	8.1806	21.9%

Table 5. Reynolds number values and experimental friction factor values for transporting guava juice in stainless-steel and acrylic pipes

Flow data		9° Bx				11° Bx			
		Reynolds number (R_e)	Calculated friction factor (f_{cal})	Experimental friction factor (f_{exp})		Reynolds number (R_e)	Calculated friction factor (f_{cal})	Experimental friction factor (f_{exp})	
Acrylic pipes	Stainless-steel pipes			Acrylic pipes	Stainless-steel pipes				
3	25	134.95	0.474	0.473	0.501	33.586	1.906	1.63	1.77
4.5	25	225.85	0.283	0.268	0.302	60.513	1.058	1.001	1.053
6	25	325.45	0.197	0.189	0.217	91.888	0.697	0.573	0.584
9	25	544.65	0.118	0.121	0.133	165.555	0.387	0.299	0.305
10.8	25	686.56	0.093	0.105	0.111	215.732	0.297	0.24	0.263
3	20	237.86	0.269	0.251	0.273	64.208	0.997	0.831	0.91
4.5	20	398.07	0.161	0.124	0.142	115.684	0.553	0.449	0.474
6	20	573.63	0.112	0.089	0.117	175.665	0.364	0.298	0.339
9	20	960.00	0.067	0.055	0.071	316.497	0.202	0.169	0.185
10.8	20	1,210.13	0.053	0.046	0.06	412.421	0.155	0.153	0.167
3	12	870.61	0.074	0.076	0.079	283.034	0.226	0.246	0.311
4.5	12	1,457.0	0.044	0.049	0.052	509.945	0.126	0.123	0.156
6	12	2,099.57	0.030	0.031	0.033	774.344	0.083	0.075	0.10
9	12	3,513.71	0.018	0.02	0.022	1,395.143	0.046	0.039	0.057
10.8	12	4,429.21	0.014	0.016	0.019	1,817.983	0.035	0.032	0.046

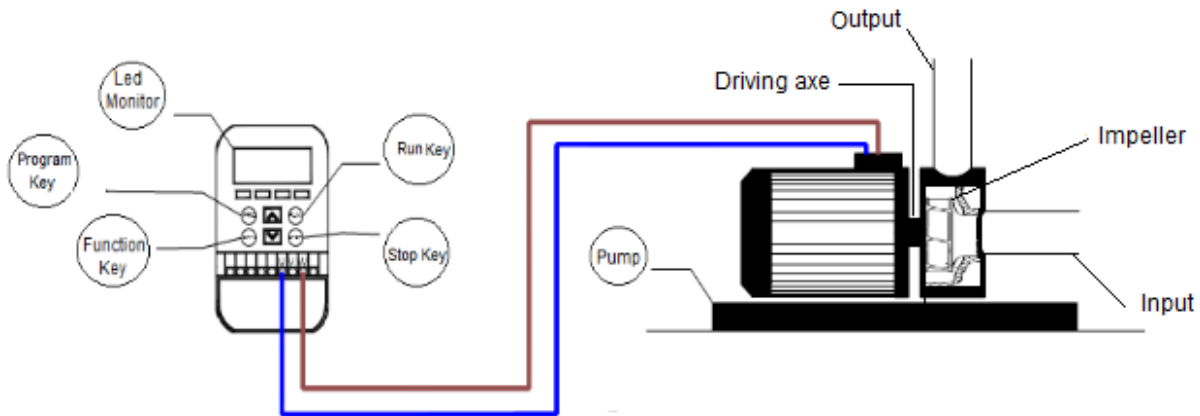


Fig 4. The method of switching the VFD with the pump motor

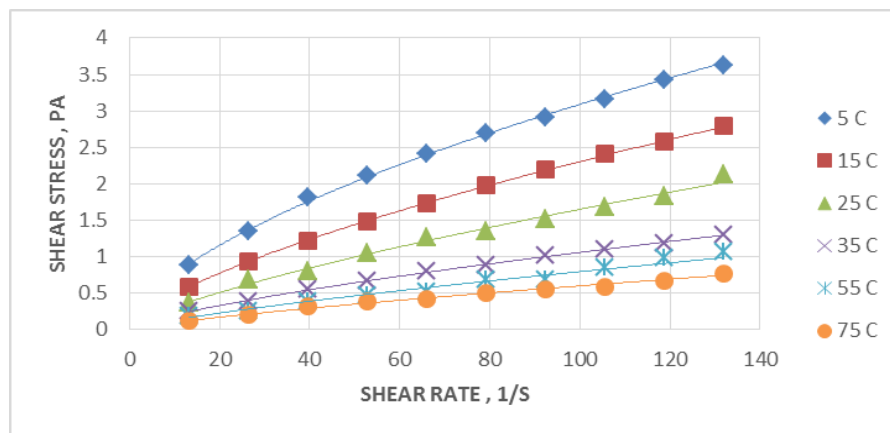


Fig 5. Shear rate and shear stress relation for 9°Bx guava juice at different temperatures

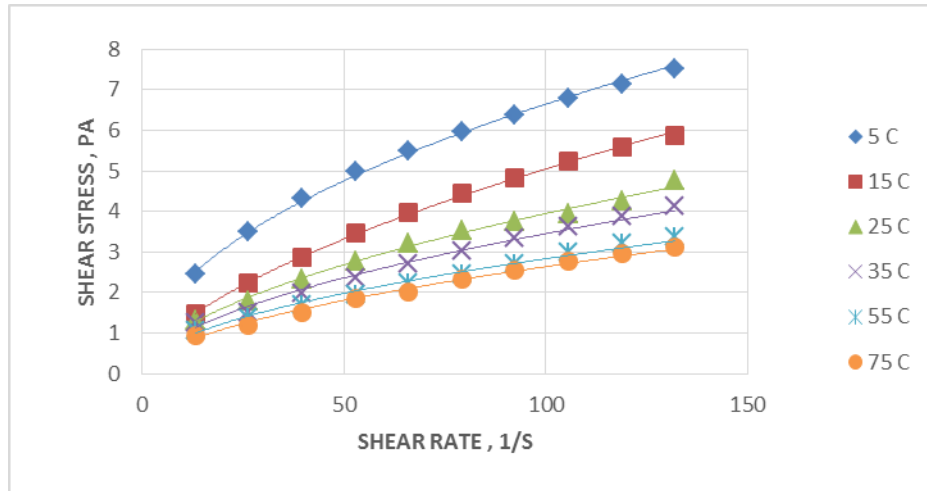


Fig 6. Shear rate and shear stress relation for 11°Bx guava juice at different temperatures

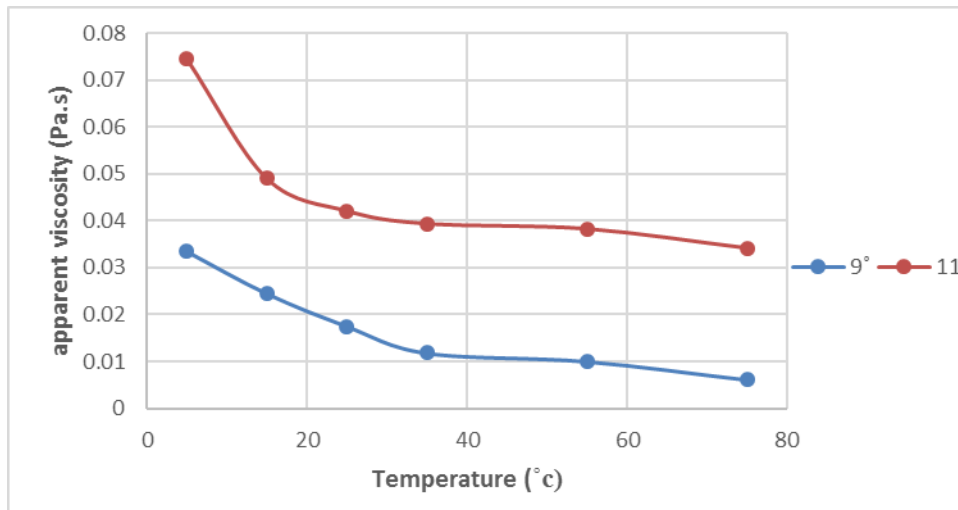


Fig 7. The influence of temperature on the apparent viscosity of guava juice (9° Bx and 11°Bx solid concentrations) at 80 S^{-1} shear rate

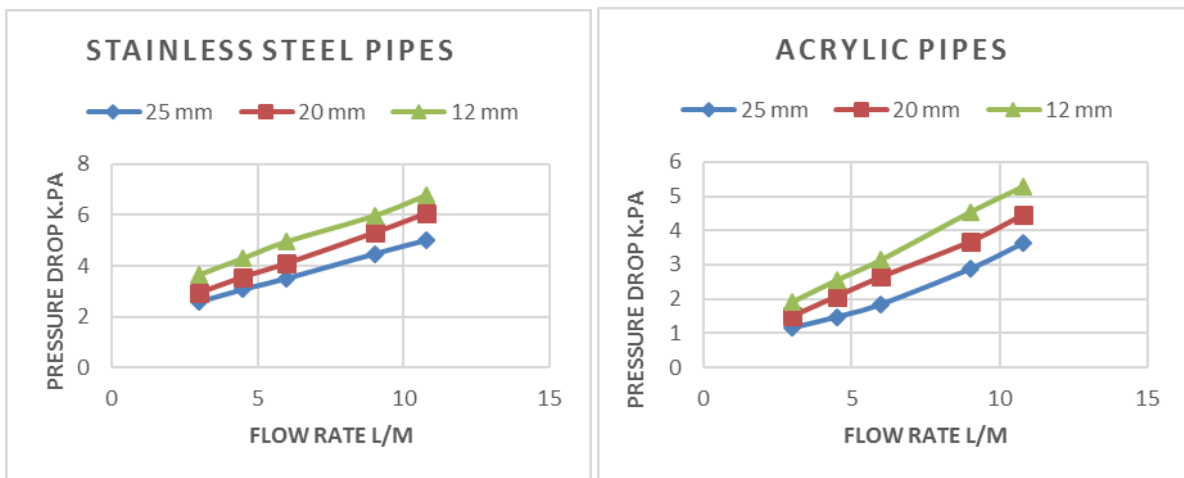


Fig 8. Variation in pressure drop across acrylic and stainless-steel pipes at different volumetric flow rates for 9°Bx of guava juice across a distance of 1.2 m.

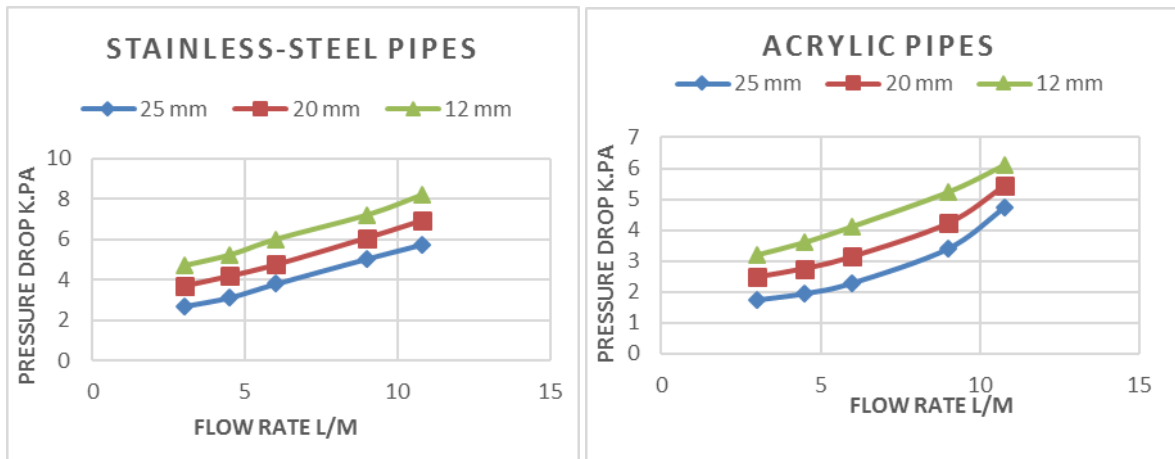


Fig 9. Variation in pressure drop across acrylic and stainless-steel pipes at different volumetric flow rates for 11° Bx guava juice across a distance of 1.2 m

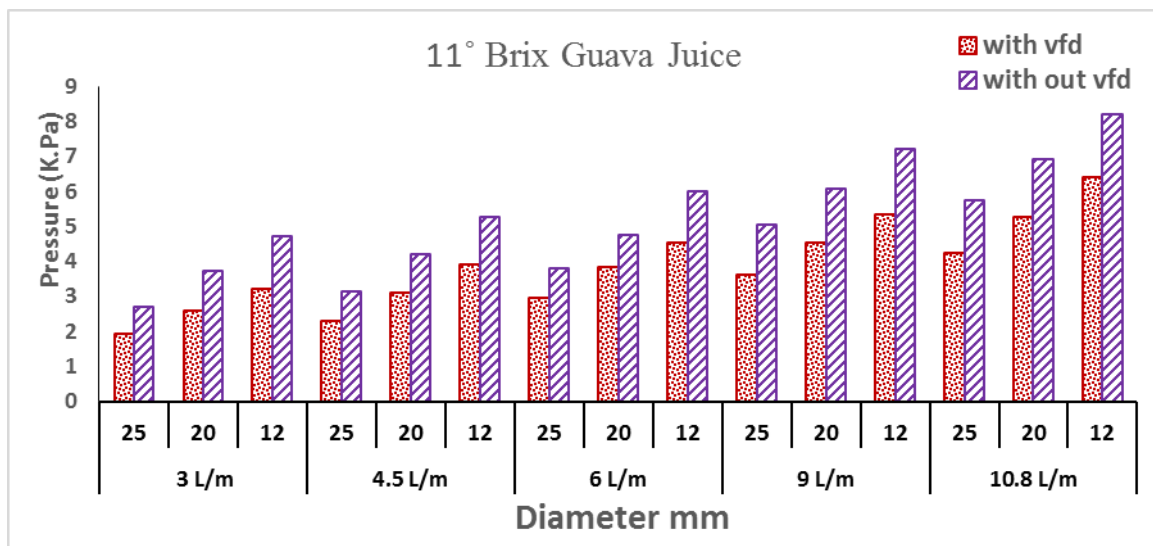


Fig 10. Variation in pressure drop across the stainless-steel pipes with different diameters at different volumetric flow rates for 11° Bx guava juice

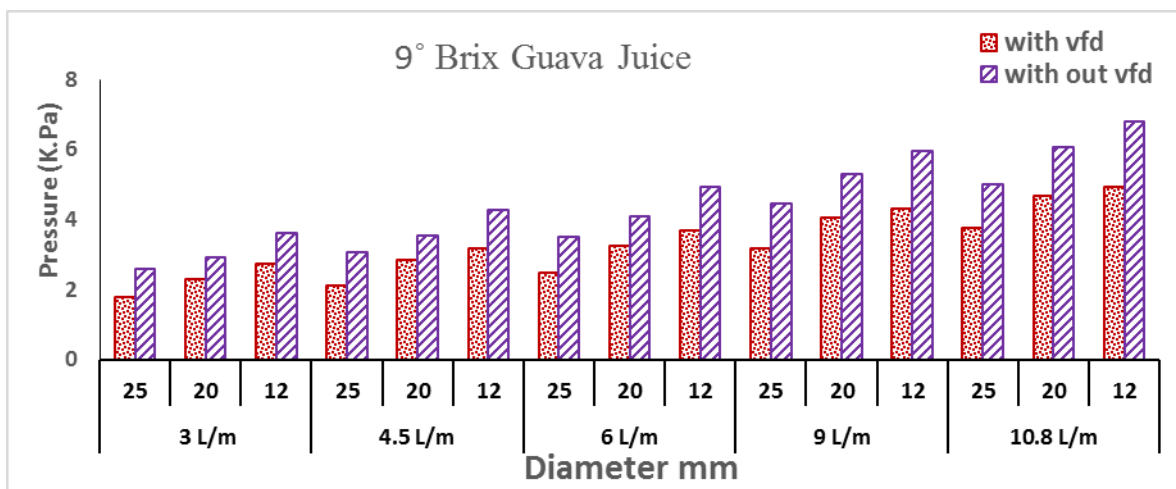


Fig 11. Variation in pressure drop across the stainless-steel pipes with different diameters at different volumetric flow rates for 9° Bx guava juice.

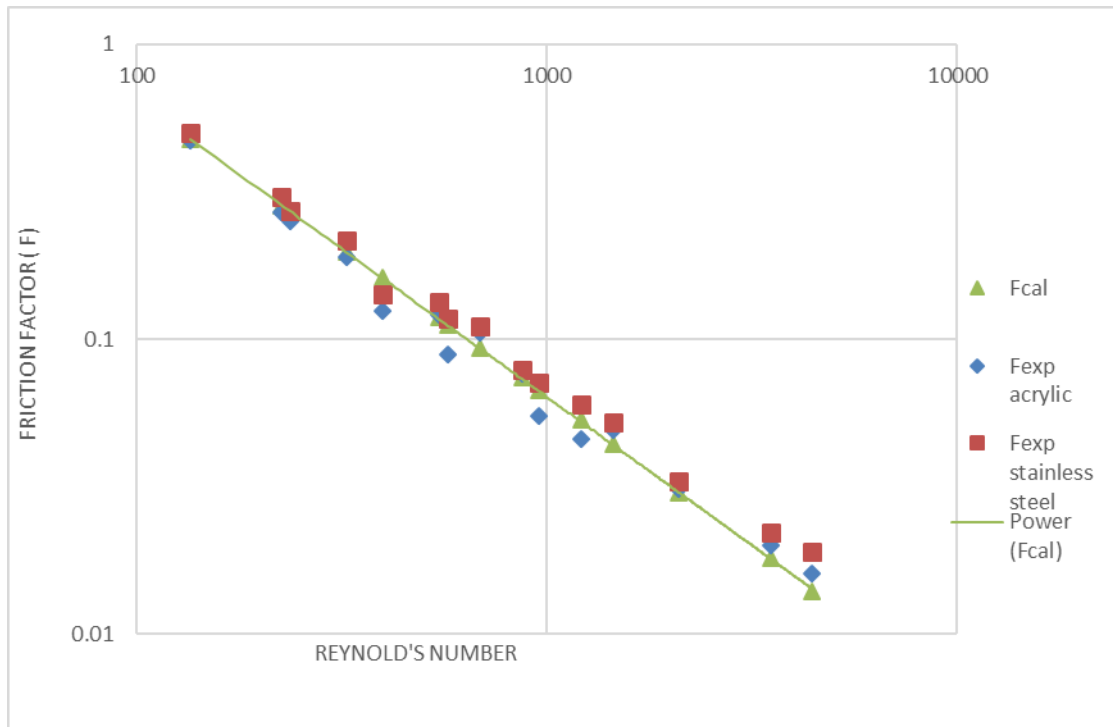


Fig 12. Reynolds number influence on friction coefficients of 9°Bx guava juice for acrylic and stainless-steel pipes

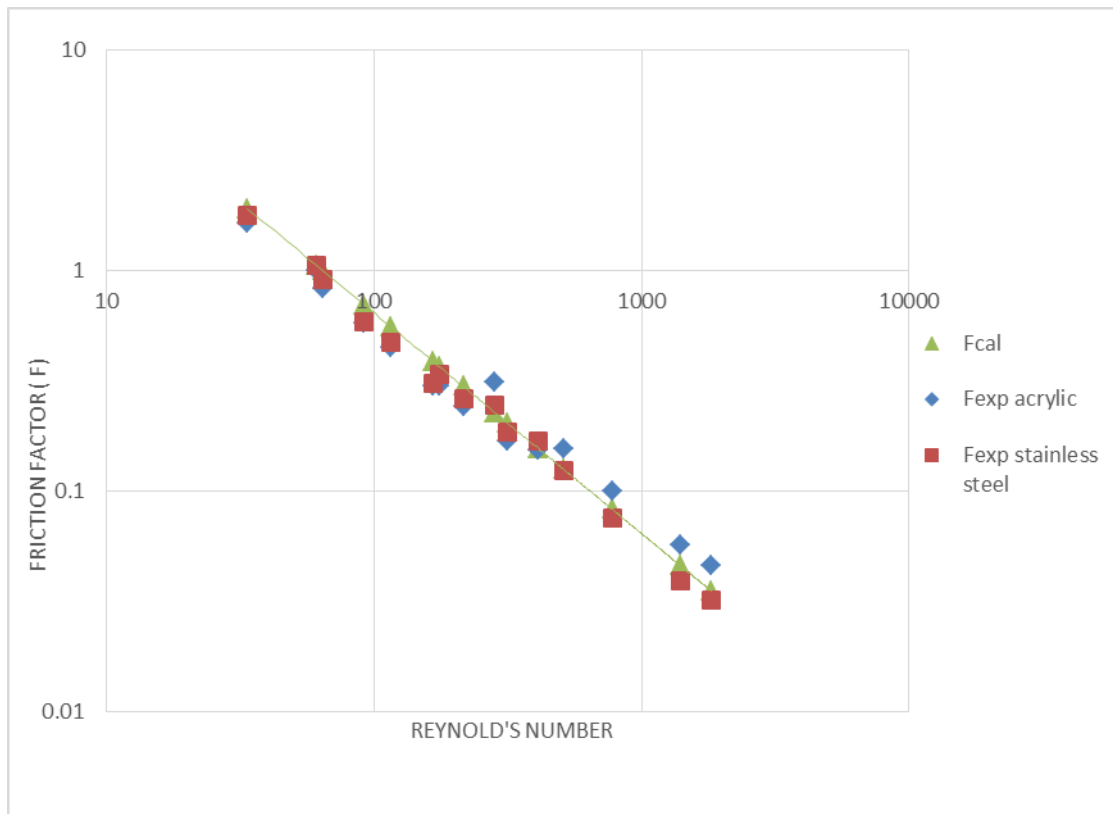


Fig 13. Reynolds number influence on friction coefficients of 11°Bx guava juice for acrylic and stainless-steel pipes

4 Conclusion

The rheological results of guava juice showed the suitability of the power law model to present the shear rate/shear stress data for 9°Bx and 11°Bx guava juice samples at temperatures from 5°C to 75°C. The behavior of the non-Newtonian flow of the juice samples required applying a generalized Reynolds number for experimentally determining the pressure drop and calculating the friction factor. The obtained n values were 0.716 and 0.543, respectively, for the 9°Bx and 11°Bx guava juice samples, indicating a higher shear-thinning effect of the more concentrated juice. Additionally, the obtained flow pattern was primarily in the laminar region. Using a VFD attached to the centrifugal pump resulted in an average of 25.73% reductions in pressure drop and the pump's total head and driving power. Furthermore, the experimental friction factor values were close to those obtained by applying the Darby equation for calculating friction values in the applied Reynolds number. Therefore, using VFD is advisable for saving pumping power in the juice industry and preventing microbial hazards from applying reduction values in the piping systems of fruit juices because of the so-called dead area formation around the valve location.

References

Abdullah N, Chin NL, Yusof YA, et al (2018) Modelling of rheological behavior of guava, pomelo and soursop juice concentrates via shear rate-temperature-concentration superpositioning. *Food Science Technology* 55, 1207–1213. <https://doi.org/10.1007/s13197-017-3024-7>

Aldi N, Buratto C, Casari N, et al (2017) Experimental and numerical analysis of a non-Newtonian fluid processing pump. *Energy Procedia* 126, 762-769. <https://doi.org/10.1016/j.egypro.2017.08.247>

Astolfi-Filho Z, Telis VRN, De Oliveira EB, et al (2011) Rheology and fluid dynamics properties of sugarcane juices, *Biochemical Engineering Journal* 53, 260–265. <https://doi.org/10.1016/j.bej.2010.11.004>

A.O.A.C (2005) Official Methods of Analysis, 18th Ed. *Association of Official Analytical Chemists Inc. USA*. http://sutlib2.sut.ac.th/sut_contents/H125800.pdf

Cabral RAF, Gut J AW, Telis VRN, et al (2010) Non-Newtonian flow and pressure drop of pineapple juice in a plate heat exchanger. *Brazilian Journal of Chemical Engineering* 27, 563 – 571. http://old.scielo.br/scielo.php?script=sci_arttext&pid=S0104-66322010000400008

Csizmadia P, Till S (2018) The Effect of rheology model of an activated sludge on to the predicted losses by an elbow. *Periodica Polytechnica Mechanical Engineering* 62, 305–311. <https://doi.org/10.3311/PPme.12348>

Darby R (2001) Chemical engineering fluid mechanics. 2nd Ed, Marcel Dekker, New York, USA. <https://rb.gy/yso84>

Earle RL (1985) Unit Operations in Food Processing 2nd Ed, Pergamon Press London, UK. <https://rb.gy/rd6dv>

Garud YY, Gole SR, Jadhav RT, et al (2016) A study on variable frequency drive and it's applications. *International Journal of Innovative Research in Science, Engineering and Technology* 5, 3079-3084. <https://api.semanticscholar.org/CorpusID:226220952>

Gratao ACA, Silveira Jr V, Telis-Romero J (2007) Laminar flow of soursop juice through concentric annuli: friction factors and rheology. *Food Engineering* 78, 1343-1354. <https://doi.org/10.1016/j.jfoodeng.2006.01.006>

Gopalkrishna PV, Kishore K, Srinivasa Rao K (2018) Comparative performance evaluation of steeped and stepless drive in turning. *Global Journal of Engineering Science and Researches* pp 29-39. <http://www.gjesr.com/Issues%20PDF/ICAME-2018/5.pdf>

Johnson M, Gul S, Vajargah AK, et al (2018) Real-time friction factor monitoring: characterization of drag reduction in polymer-based fluids, *American Association of Drilling Engineers*, Houston. <https://www.aade.org/application/files/3015/7131/7049/AADE-18-FTCE-118 - Johnson.pdf>

Metzner B, Reed JC (1955) Flow of non-Newtonian fluids – correlation of the laminar, transition, and turbulent-flow regions. *American Institute of Chemical Engineers* 4, 434-440. <https://doi.org/10.1002/aic.690010409>

Neuberger T, Weston SB (2012) Variable frequency drives: energy savings for pumping applications. *Industry Application*, Publication No. IA04008002E / Z12581, Eaton Corporation. <https://rb.gy/t0x14>

Prajapati H, Arya S, Baria J (2019) Variable Frequency Drive. *SSRN Electron Journal*. <http://dx.doi.org/10.2139/ssrn.3442439>

Quek MC, Chin, NL, Yusof, Y (2013) Modelling of rheological behavior of soursop juice concentrates using shear rate-temperature-concentration superposition. *Food Engineering* 118, 380–386. <https://doi.org/10.1016/j.jfoodeng.2013.04.025>

Sahin S, Sumnu SG (2006) Rheological properties of foods. In: *Physical Properties of Foods. Food Science Text Series*. Springer, New York, NY. https://doi.org/10.1007/0-387-30808-3_2

Sorgun M, Ulker E (2020) Friction factor calculation for turbulent flow in annulus with temperature effects, *International Journal of Numerical Methods for Heat and Fluid Flow* 30, 3755-3763. <https://doi.org/10.1108/HFF-07-2019-0578>

Sugai AY (2002) Processamento descontínuo de purê de manga (*Mangifera indica* Linn) variedade Haden: estudo da viabilidade do produto para pronto consumo. MS thesis, São Paulo, Brazil. Universidade de São Paulo, Chemical Engineering Department. <https://doi.org/10.11606/D.3.2002.tde-05052003-151029>

Tahara C (2016) VFDs: An alternative to valves for mechanical throttling. *Process Instrumentation*. <https://rb.gy/idq8j>

Taler D (2016) Determining velocity and friction factor for turbulent flow in smooth tubes. *International Journal of Thermal Sciences* 105, 109-122. <https://doi.org/10.1016/j.ijthermalsci.2016.02.011>

Tamminen J, Viholainen J, Ahonen T, et al (2014) Comparison of model-based flow rate estimation methods in frequency-converter-driven pumps and fans. *Energy Efficiency* 7, 493–505. <https://doi.org/10.1007/s12053-013-9234-6>

Yuan X, Tao Z, Li H, et al (2016) Experimental investigation of surface roughness effects on flow behavior and heat transfer characteristics for circular microchannels. *Chinese Journal Aeronaut* 29, 1575–1581. <https://doi.org/10.1016/j.cja.2016.10.006>

Zainal BS, Abdul Rahman R, Ariff AB, et al (2000) Effects of temperature on the physical properties of pink guava juice at two different concentrations. *Journal of Food Engineering* 43, 55–59. [https://doi.org/10.1016/S0260-8774\(99\)00132-6](https://doi.org/10.1016/S0260-8774(99)00132-6)